LA-UR-14-28944 (Accepted Manuscript)

Testing the Delayed Gamma Capability in MCNP6

Weldon, Robert Allen Jr.
Fensin, Michael Lorne
Mckinney, Gregg Walter

Testing the Delayed Gamma Capability in MCNP6

R. A. Weldon Jr., M. L. Fensin*, G. W. McKinney

Los Alamos National Laboratory, MS-C921, Los Alamos, NM 87545
Tel: +1 505 606 0145, Fax: +1 505 665 2897, Email: mfensin@lanl.gov

Send proofs and invoice to:
Dr. Michael Lorne Fensin
Los Alamos National Laboratory
MS-C921, Los Alamos, NM 87545
mfensin@lanl.gov

Page Count: 24 Pages including cover
Figures

1 Figure and 4 Tables.

Testing the Delayed Gamma Capability in MCNP6

R. A. Weldon Jr., M. L. Fensin, G. W. McKinney

Abstract – *The mission of the Domestic Nuclear Detection Office is to quickly and reliably detect unauthorized attempts to import or transport special nuclear material for use against the United States. Developing detection equipment to meet this objective requires accurate simulation of both the detectable signature and detection mechanism. A delayed particle capability was initially added to MCNPX 2.6.A in 2005 to sample the radioactive fission product parents and emit decay particles resulting from the decay chain. To meet the objectives of detection scenario modelling, the capability was designed to sample a particular time for emitting particular multiplicity of a particular energy. Because the sampling process of selecting both time and energy is interdependent, to linearize the time and emission sampling, atom densities are computed at several discrete time steps, and the time integrated production is computed by multiplying the atom density by the decay constant and time step size to produce a cumulative distribution function for sampling the emission time, energy and multiplicity. The delayed particle capability was initially given a time bin structure to help reasonably reproduce, from a qualitative sense, a fission benchmark by D. Beddingfield, which examined the delayed gamma emission. This original benchmark was only qualitative and did not contain the magnitudes of the actual measured data, but did contain relative graphical representation of the spectra. A better benchmark with measured data was later provided by A. W.Hunt, Vladimir Mozin, E.T.E. Reedy, H.A. Selpel and* Steve *Tobin at the Idaho Accelerator Center; however, due to the complexity of the benchmark setup, sizable systematic errors were expected in the modeling, and initial results compared to MCNPX 2.7.0 showed errors outside of statistical fluctuation. Presented here is a more simplified approach to benchmarking, utilizing closed form analytic solutions to the granddaughter equations for*

particular sets of decay systems. We examine five different decay chains (two stage decay to stable), and show the predictability of the MCNP6 delayed gamma feature. Results do show that while the default delayed gamma calculations available in the MCNP6 1.0 release can give accurate results for some isotopes (e.g. Ba-137), the percent differences between the closed form analytic solutions and the MCNP6 calculations were often greater than 40% (Mg-28, Al-28, K-42, Ca-47, Sc-47, Co-60). With the MNCP6 1.1 Beta release, the 10th entry on the DBCN card allows improved calculation within less than 5% as compared to the closed form analytic solutions for immediate parent emissions and transient equilibrium systems. While the 10th entry on the DBCN card for MCNP6 1.1 gives much better results for transient equilibrium systems and parent emissions in general, it did little to improve daughter emissions of secular equilibrium systems. Hypotheses were presented as to why daughter emissions of secular equilibrium systems might be mispredicted in some cases and not in others.

KEYWRODS: MCNP6, Delayed Gamma, Activation

I. INTRODUCTION

The mission of the Domestic Nuclear Detection Office (DNDO) is to quickly and reliably detect unauthorized attempts to import or transport special nuclear material (SNM) for use against the United States. Developing detection equipment to meet this objective requires accurate simulation of both the detectable signature and detection mechanism. MCNP6 is capable of transporting the various types of radiation encountered in these scenarios; however, the accuracy of MCNP6 must be quantified such that we can be confident in the results of the simulations. Delayed gamma transport is one important component of these detection scenarios. In the context

of this paper, delayed gamma transport is defined as the combination of gamma emission from the decay of radioactive isotopes and the subsequent transport of that gamma radiation through matter.

Cross section processing codes (like NJOY),[1] are used to produce a more compact file organization of the Evaluated Nuclear Data Files (ENDF) called ACE (**A C**ompact **E**NDF).[2] The ACE file format is read by MCNP in order to load cross section and secondary particle emission information. At the top of each ACE file entry for each actinide are a series of pointers exists that describe either the amount of something (the nxs() array) or the location of something (the jxs() array). For continuous energy actinide cross sections for actinides, the 8th entry of the nxs() array stores the number of delayed neutron precursor families while 21-24th entries of the jxs() array point to locations for storing the fission cross section and delayed neutron emission information. MCNP always possessed the ability to emit delayed neutrons from fission; however, these delayed neutron spectra and intensity were functional fits stored with the actinide cross sections and not directly sampled from the created fission products. Furthermore, there existed no method to emit the decay photons from radioactive fission products (or any radioactive nucleus).

A delayed particle capability was initially added to MCNPX 2.6.A in 2005 to sample the radioactive fission product parents and emit decay particles resulting from the decay chain.[3] At the point of capture, a residual nucleus is created and decayed using the CINDER90 depletion code.[4] The CINDER90 depletion code solves the BATEMAN equations displayed in Eq. 1a-c.

$$\frac{dN_m(t)}{dt} = -N_m(t)\beta_m + \sum_{k\neq m} N_k(t)\gamma_{k\rightarrow m} \quad (1a)$$

$$\beta_m = \lambda_m + \sum_r \int \sigma_{m,r}(E)\Phi(E,t)dE \quad (1b)$$

$$\gamma_{k\to m} = \sum_{k\neq m} L_{k\to m}\lambda_k + \sum_{k\neq m}\sum_r \int Y_{k\to m,r}\sigma_{k,r}(E)\Phi(E,t)dE \quad (1c)$$

Where $N_m(t)$ is the concentration of isotope m, β_m is the destruction coefficient for isotope m, $\gamma_{k\to m}$ is the creation coefficient of isotope k transmuting/decaying into isotope m, λ_m is the decay constant for isotope m, $\sigma_{m,r}(E)$ is the energy dependent cross section of reaction r for isotope m, $\Phi(E,t)$ is the energy and time dependent scalar flux, $L_{k\to m}$ is the probability of decaying from isotope k to isotope m given that isotope k has decayed, and $Y_{k\to m,r}$ is the transition probability of isotope k to isotope m given that reaction r has taken place.

MCNP only sends CINDER90 a residual radioactive nucleus and not a flux (i.e. capture rate). As a result, the capture terms ($\sum_r \int \sigma_{m,r}(E)\Phi(E,t)dE$ and $\sum_{k\neq m}\sum_r \int Y_{k\to m,r}\sigma_{k,r}(E)\Phi(E,t)dE$) are removed from the destruction and creation coefficients resulting in Eq. 1a being a set of coupled first order differential equations with constant coefficients (where the coupling comes from the production coefficient $\gamma_{k\to m}$). Theoretically, these equations could be solved analytically; however, CINDER90 employs a numerical Markov linear chain scheme to solve these equations.

The delayed particle capability samples not only the energy and multiplicity of the emission but also the time in which the radioactive nuclide decays and emits decay particles. As a result, a cumulative distribution function (CDF) must be generated to sample when in time the particle is emitted based on total emission activity at various times, and another CDF is required to determine the emission probability of a particular energy at the sampled time. The probability of sampling a single gamma energy emission, from a collection of isotopes, at a particular time is

$$p_\gamma(i,E,t) = \frac{\lambda_i N_i(t=t') * B_{\gamma,i} * P_{E',i}}{\sum_i \sum_E \lambda_i N_i(t=t') * B_{\gamma,i} * P_{E',i}} \tag{2}$$

Where $p_\gamma(t,E,I)$ is the probability of emitting a decay gamma of energy E from isotope i at time t, λ_i is the decay constant of isotope i, $N_i(t=t')$ is the time dependent atom density evaluated at time t', $B_{\gamma,i}$ is the branching ratio for gamma decay given that isotope i has decayed, and $P_{E',i}$ is the probability of emitting energy E from isotope i given that a gamma decay will occur. The probability of sampling a time to emit a single gamma energy, from a single isotope decay, at a particular time is

$$p_{\gamma,i,E}(t)dt = \lambda_i N_i(t') * B_{\gamma,i} * P_{E',i} * e^{-\lambda_i t} dt \tag{3}$$

Therefore the sampling for a single line, for a single isotope decay to a stable daughter, requires only

$$t = \frac{-\ln(\xi)}{\lambda} \tag{4}$$

Most residuals have daughters, granddaughters, etc. that can be created from several decay paths. Because the delayed particle capability must sample both time and energy (and multiplicity) the sampling requires the evaluation of Eq. 5

$$p_\gamma(i,E,t) = \frac{\int_0^t \lambda_i N_i(t') * B_{\gamma,i} * P_{E',i} * e^{-\lambda_i t} dt'}{\int_0^\infty \sum_i \sum_E \lambda_i N_i(t') * B_{\gamma,i} * P_{E',i} * e^{-\lambda_i t} dt'} \quad (5)$$

Unfortunately, the probability of emitting a gamma in time depends on the time dependent atom density, which changes with isotope decay, making the sampling nonlinear. CINDER90 can only calculate the time dependent activity at discrete times, and even if a continuous function could be developed, running CINDER90 for each interaction is expensive.

To combat this solution difficulty, the CDF for time sampling for a particular residual is generated by determining the ratio of the time integrated production up to a particular time divided by the time integrated production over all time. A trapezoidal rule is used to numerically determine the time integrated delayed-gamma production.[5] In short, atom densities are computed at several time steps, and the time integrated production is computed by multiplying the atom density for the time step by the decay constant (λ), the gamma yield and duration of time steps (dt). The major assumption here is that the atom density over the time step does not significantly vary "enough." The loose definition of "enough" is related to the fact that a rectangle is now used to approximate the area under the function of atom density vs. dt. For a burnup reactivity calculation, this assumption usually works great for reasonable time steps as burnup is dependent upon changing the nuclide concentration enough to change the flux;[6] however, for radioactive decay emission (where flux is now eliminated), the decay rate may significantly change over a time step depending upon the time step length and half-life of the isotope.

The delayed particle capability was initially given a time bin structure to help reasonably reproduce, from a qualitative sense, a fission benchmark by D. Beddingfield, which examined the delayed gamma emission.[7] This original benchmark was only qualitative and used to identify

whether or not certain decay lines were being produced. The benchmark did not contain the magnitudes of the actual measured data, but did contain relative graphical representation of the spectra.[7] A better benchmark with measured data was later provided by A. W.Hunt, Vladimir Mozin, and Steve Tobin at the Idaho Accelerator Center.[8] The benchmark included using an electron accelerator to produce photons in a tungsten converter, which then irradiated a beryllium cylinder to produce neutrons that interrogated the actinide targets. After 1 hour of irradiation, the actinide targets were moved to a separate geometry for counting the decay gammas with high purity germanium detectors. Due to the complexity of the setup, it was expected that there would be a sizable amount of systematic error in the modeling, and initial results compared to MCNPX 2.7.0 showed error outside of statistical fluctuation. T. A. Wilcox, M. L. Fensin, E. Pierce, V. Mozin, J. W. Durkee, A. W. Hunt, and G.W. McKinney later tested several new trapezoidal time bin structures to quantify the relative improvement of the various time binning setups on the delayed photon emission.[9] For MCNP6, G. W. McKinney enhanced the time bin structure by going from 100 to 234 bins where the bin structure ranged, by decade, from 1e-6 to 9e19 (to be released in MCNP6 1.1 Beta). Since prior benchmarking focused on complex isotope decay systems (because of the plethora of decay chains generated from fission), difficulty existed in attempting to isolate fundamental deficiencies in the method. Furthermore, because complex setups were used to irradiate samples in one geometry while counting them in another, it was even more difficult to isolate whether there was systematic bias based on modeling simplifications.

Addressed here is a more simplified approach to benchmarking in order to best assess: (1) whether or not deficiencies exist in the current methodology for certain types of decay chains; and (2) paths forward for improving the delayed particle emission capability. We utilize closed form

analytic solutions to the granddaughter equations for particular sets of isotope systems to compare the accuracy of the delayed gamma capability in MCNP6.

II. THEORY

Radioactive nuclides can decay by spontaneous fission or the emission of several different particle types such as: alphas, betas, gammas and/or neutrons. Here we focus on simple beta and gamma decay. The decay chain from an unstable grandparent to a stable daughter can be written mathematically in what are called the granddaughter equations. Giving that the starting parent nuclide is radioactive, the loss of the parent nuclide is proportional to the negative product of the parent population and the decay constant

$$\frac{dN_A}{dt} = -\lambda_A N_A \tag{6}$$

The gain of the daughter nuclide is proportional to the loss of the parent minus the product of the population of the daughter and decay constant

$$\frac{dN_B}{dt} = \lambda_A N_A - \lambda_B N_B \tag{7}$$

Because the granddaughter is stable, the granddaughter can only be gained by loss of the daughter nuclide

$$\frac{dN_C}{dt} = \lambda_B N_B \tag{8}$$

The solutions to the time dependent atom densities of the parent (Eq. 9a), daughter (Eq. 9b) and granddaughter (Eq. 9c) then become

$$N_A = N_0 e^{-\lambda_A t} \tag{9a}$$

$$N_B = \frac{\lambda_A N_0}{\lambda_A - \lambda_B}\left(e^{-\lambda_B t} - e^{-\lambda_A t}\right) \tag{9b}$$

$$N_C = \frac{\lambda_B \lambda_A N_0}{\lambda_A - \lambda_B}\left(\frac{e^{-\lambda_B t} - 1}{\lambda_B} - \frac{e^{-\lambda_A t} - 1}{\lambda_A}\right) \tag{9c}$$

Using the granddaughter equations, the total emission of a particular gamma energy, from a particular isotope, over a given dt can be calculated by

$$Emission_i = B_{\gamma,i} P_{E',i} \int_0^t N_i(t) dt \tag{10}$$

Using the solutions to the governing equations, the integral can be calculated for the number of emissions over time by

$$Emission_A = B_{\gamma,A} P_{E',A}\, \lambda_A N_0\left(1 - e^{-\lambda_A t}\right) \tag{11}$$

$$Emission_B = \frac{B_{\gamma,B} P_{E',B} \mathrm{N}_0\left(\lambda_A\left(1 - e^{-\lambda_B t}\right) + \lambda_B\left(e^{-\lambda_A t} - 1\right)\right)}{\lambda_B(\lambda_A - \lambda_B)} \tag{12}$$

III. METHOD

To test the delayed gamma capability, MCNP6 calculations were compared with the closed form analytic solutions for the particular gamma emissions. The cindergl.dat library file contains all the ENDF/B decay data sub-library information used by the code for computing delayed gamma emissions. Several isotopes were chosen from cindergl.dat for testing. The isotopes were chosen based on the following criteria: (1) the isotopes was available in cindergl.dat; (2) the isotope possessed 2 stage decay, by beta emission, to a stable granddaughter isotope; (3) the isotopes had fewer than 100 gamma emission lines; (4) the (n,n') interactions of the parent, also resulting in a radioactive nucleus, did not have overlapping decay lines with other nuclei in the decay chain; and (5) the decay chains chosen must have had at least 1 transient and 1 secular equilibrium decay chain. Table I displays the selected isotopes based on the above criteria.

Of the several isotopes in cindergl.dat that met the selected criteria, four were in secular equilibrium and one was in transient equilibrium. Secular equilibrium is defined as when a nuclide decays from a parent with a relatively long half-life to a daughter with a relatively short half-life. Transient equilibrium is when the parent and daughter have half-lives of similar length, where the parent half-life is only slightly larger.

Individual input decks were created for each parent isotope. The decks were set with neutrons being isotropically emitted from the origin at an energy of 1 MeV. A sphere centered at the origin with a radius of 1e-6 cm was made of an isotope with one less neutron than the parent isotope being investigated. An ACT card was used to sample delayed gammas using CINDER90 based on line emission data (as opposed to pure multi-group data). The options used were FISSION=NONE which causes no delayed particles to be produced from fission events (which should be irrelevant for nonactinides), NONFISS=P which creates delayed gammas from non-

fission events, and DG=LINES which samples delayed gammas using models based on line-emission data augmented by 25-group data from CINDER90.[10] The LCA 7j -2 option was used to ensured that the neutrons immediately collide, and all progeny escapes without further interactions; therefore the size and density of the sphere are irrelevant, and hence the results can now be normalized per (n,γ) interaction leading to decay. Surface current tallies with time bins were used to record the emissions. The energy range was set between 0 and 6 MeV with 1 keV bins. The time bins were set to record two time periods: (1) from 0 to 1e3 shakes to account for prompt gammas; and (2) from 1e3 to max time to account for delayed gammas. To account for the different gamma emission times, five time bins were used for tallying. These times were 1 minute, 1 hour, 1 day, 1 year, and 100 years. The ft8 RES option was used to tally the (n,γ) interactions versus other interactions. This was necessary in order to achieve photon tally results per decay, instead of per source neutron. To obtain the result per decay, we divided the photon tally by the ft8 RES (n,γ) interaction result.

Fig. 1 displays and example decay chain for Mg-28 to Si-28, by way of activation of Mg-27. Notice that the activation of Mg-27 results in the creation of Mg-28, which by way of 2 stage beta decay reaches stable Si-28. Because Mg-27 is radioactive, there exists the possibility that an immediate reaction will result in (n,n'). An (n,n') reaction still results in the radioactive nucleus of Mg-27, which would be sent to CINDER90 for decay. Because Mg-27 does not contain energy emissions that overlap with those of Mg-28 or Al-27, based on the tally criteria given above, this decay system is favorable as a benchmark; otherwise we would be incorrectly comparing analytical results to MCNP computation due to double counting overlapping bins. It is true that we could have chosen a tighter criteria than 1 keV bins; however, this criteria is reasonably typical for HPGE detectors.[11]

Using this setup, three sets of calculations were performed. The first was performed with 1e8 particles using MCNP6 1.0, the second was performed with 1e9 particles using MCNP6 1.0, and the third was performed with 1e8 particles using MCNP6 1.1 Beta and made use of the tenth entry on the DBCN card (the DBCN card is the debug information card used primarily for debugging the code itself and implementing specialty features not available on other MCNP cards), which allows for a more refined time-binning structure (from 100 to 234 bins) when the stability half-life is specified to be greater than 1.5768e16 s. Because emitting a delayed gamma involves constructing a sampling CDF based on emission probabilities, and these probabilities can vary significantly in magnitude, the first two cases provide a comparison of how the accuracy of the delayed gamma capability increases as more particles were run resulting in a better sampling of the entire emission probability. The third case was used to test the new time-binning structures available through use of the DBCN card in MCNP6 1.1 Beta. Appendix A contains an example of the Mg-28 decay chain emission calculation.

IV. RESULTS

Tables II-IV shows the percent difference (MCNP/Analytic-1) for the three MCNP6 calculation types, as compared to the analytic solutions, for each examined decay system. For MCNP6 1.0 using 1e8 starting histories, Mg-28 consistently overpredicted the highest at over ~125% for each emission line and time. Al-28 and K-42 were consistently underpredicted by ~40%-50% while Ca-47 was consistently overpredicted by ~57%. These three nuclides all had half-lives ranging from a few minutes to a few days (Al-28→2.25 minutes; K-42→13.36 hours; Ca-47 → 4.536 days), and the misprediction was consistent for all 5 time integrations. Sc-47

showed accurate results for shorter times with percent differences of ~5.7% for 1 hour and 4.0% for 1 day, but at later times the percent differences grew to 49.3% for both 1 year and 100 years. If the half-life of the single isotope alone was the driver in accuracy, Sc-47, with a half-life of 3.349 days, should have had the same absolute value of accuracy as Al-28, K-42 and Ca-47 (or same magnitude as Ca-47); however, this was not the case. At 100 years the percent difference for Co-60's emission lines were -55.1% for 1.17 MeV and -55.8% for 1.33 MeV. The most accurate results were for Ba-137 with percent differences of -3.74%, -6.03%, -5.55%, and -3.30% for times 1 hour, 1 day, 1year, and 100 years respectively.

MCNP6 1.0 using 1e9 starting histories had very similar results For MCNP6 1.0 using 1e8 starting histories. The only major difference between the two cases was that for NPS 1e9 more emission lines were recorded at shorter times. For Sc-47 and Ba-137 emissions were recorded at 1 minute. Additional emissions were also recorded for K-42 at 1 day and Co-60 at 1 year (for the 1.17 MeV emission line).

As compared to using MCNP6 1.0, using MCNP6 1.1 with the 10^{th} energy of the DBCN card, showed considerable improvement for several of the isotopes. The largest improvements were seen for Mg-28, Ca-47, and Sc-47. For Mg-28 the percent differences decreased from ~125% for all emission lines and times to ~3% for all emission lines and times. For Ca-47 the percent differences decreased from ~56% for all emission lines and times to ~4%. Sc-47 also showed considerable improvement over the other two sets of calculations with percent differences of 0.43%, 0.06%, 4.64%, and 4.64% for 1 hour, 1 day, 1 year, and 100 years respectively. Al-28, K-42, Co-60, and Ba-137 showed only small changes from the first two sets of calculations. The only difference of note was that Al-28 the percent differences at 1 year and 100 years was ~6% worse than the MCNP6 1.0 1e8 history case.

The transient equilibrium case (Ca-47 → Sc-47 → Ti-47) had excellent agreement for the parent and daughter emission; however, 3 out of 4 of the secular equilibrium cases had excellent agreement of the parent emission but poor agreement of the daughter emission. The time integration algorithm multiplies the emission activity at time t by the dt to the next time step to compute the time integrated activity. As a result, the rectangles used to approximate the area under the curve are expected to slightly underpredict the buildup. Since the daughter did not exist at t=0, the daughter was built in as a function of time; therefore the fact that 3 out of 4 secular equilibrium

daughter emissions underpredict may have been related to the implicit calculation of the integral (therefore possibly inferring that a midpoint approach may compute a better result). However, if the implicit integration approach was supposedly underpredicting the buildup of the daughter, why was parent emission not severely overpredicted? Both Mg-28 and Ca-47 emissions were slightly overpredicted; however, the percent of overprediction of the parent emission is much less than the percent of underprediction of the daughter emission. Furthermore, the Ba-137m system seems to predict daughter emission quite well (only slightly underpredicted). Therefore these benchmarks do isolate that there is a problem in prediction of secular equilibrium decay systems; however, some unique aspect of the Ba-137m secular equilibrium system allows improved prediction as compared to the other tested secular equilibrium cases. Because the half-life of Ba-137m is very short compared with Cs-137, it might be possible that bin length at the Cs-137 decay (resulting in Ba-137m) encapsulates the entire decay of Ba-137m in one bin, leading to better prediction (this hypothesis will require further testing). The time integration scheme is outside the running of CINDER90; therefore the fact that Al-28, Co-60 and K-42 mispredicted by the same percent whether or not the 10^{th} entry on the DBCN card was used, and the parent emissions of these nuclides had improved prediction by using the 10^{th} entry on the DBCN card, is related to how the time integrated activity is calculated and not how the decay chain is treated in CINDER90.

V. CONCLUSIONS

In this paper the delayed gamma capability was benchmarked by comparison with analytic solutions. While the default delayed gamma calculations, available in the MCNP6 1.0 release, gave accurate results for some isotopes (e.g. Ba-137m), the percent differences between the analytic solutions and the MCNP6 1.0 calculations were often greater than 40% (Mg-28, Al-28,

K-42, Ca-47, Sc-47, Co-60). With the MNCP6 1.1 Beta release, the 10th entry on the DBCN card can be used to refine the time-binning structure from 100 bins to 234 bins. This new capability yields accurate results for several isotopes. Mg-28, Ca-47, and Sc-47 all had percent differences of less than 5% when compared to the closed form analytic solutions. While the 10th entry on the DBCN card gives much better results for transient equilibrium systems and parent emissions in general, it does little to improve daughter emissions of secular equilibrium systems. Al-28, K-42, and Co-60 showed very little change in their percent differences with the addition of the 10th entry on the DBCN card. Hypotheses were presented as to why daughter emissions of secular equilibrium systems might be mispredicted in some cases and not in others; however, this paper only tests released capability, and therefore future work will focus on assessing these new hypothesis for improving predictability. The MCNP6 delayed particle capability can be accurate for prediction of certain decaying isotopes; however, before using the values calculated by the delayed gamma capability a check should always be performed, using analytic solutions if possible, to ensure the accuracy of the calculation.

VI. ACKNOWLEDGEMENTS

This work was sponsored by the U.S. Department of Homeland Security, Domestic Nuclear Detection Office, under competitively awarded contract/IAA HSHQDC-12-X-00251. This support does not constitute an express or implied endorsement on the part of the Government.

VII. REFERENCES

1. A. C. KAHLER, D. W. MUIR, R. M BOICOURT, R. E. MACFARLANE, "The NJOY Nuclear Data Processing System, Version 2012," *Los Alamos National Laboratory Reprot: LA-UR-12-27079* (August 2013).

2. A. TRKOV, M. HERMAN and D. A. BROWN, “ENDF-6 FORMATS Manual,” *Brookhaven National Laboratory Report: BNL-90365-2009* Rev.2 (October 2012).

3. J. S. HENDRICKS, G. W. MCKINNEY, H. R. TRELLUE, J. W. DRUKEE, T. L. ROBERTS, H. W. EGDORF, J. P. FINCH, M. L. FENSIN, M. R. JAMES, D. B. PELOWITZ, L. S. WATERS, and F. X. GALLMEIER, “MCNPX, Version 2.6.A,” *Los Alamos National Laboratory Report: LA-UR-05-8225* (2005).

4. W. B. WILSON, V. DYADECHKO, T. R. ENGLAND, P. MOLLER, H. R. TRELLUE, “A Manual for CINDER90 Version 06.1 Codes and Data,” *Los Alamos National Laboratory Draft Report, Los Alamos*, NM (2006).

5. J. W. DURKEE, Jr., M. R. JAMES, G. W. MCKINNEY, H. R. TRELLUE, L.S. WATERS, W. B. WILSON, “Delayed-gamma signature calculation for neutron-induced fission and activation using MCNPX, Part I: Theory,” *Progress in Nuclear Energy*, **51**, pgs. 813-827 (2009).

6. M. L. FENSIN, J. S. HENDRICKS, S. ANGHAIE, “The Enhancements and Testing for the MCNPX 2.6.0 Depletion Capability,” *Journal of Nuclear Technology*, **170**, pp. 68-79 (April 2010).

7. D.H. BEDDINGFIELD, F.E. CECIL, “Identification of fissile material from fission product gamma-ray spectra,” *Nuclear Instruments and Methods in Physics Research A*, **417** (1998) 405-412.

8. V. MOZIN., S. J. TOBIN, A. W. HUNT, J. VUJIC, “Delayed Gamma Technique for Fissile Material Assay,” Proceedings of the Institute of Nuclear Materials Management 51st Annual Meeting (2010).

9. T. WILCOX, M. L. FENSIN, E. PIERCE, V. Mozin, J. W. Durkee, A. W. Hunt, G.W. McKinney, "MCNP6 Delayed Gamma Benchmark Using Experimental Data,” *American Nuclear Society: 2011 Annual Meeting*, Hollywood, Florida, (June 26-30, 2011).

10. D. B. PELOWITZ et al. “MCNP6 User’s Manual Version 1.0,” *Los Alamos National Laboratory Report: LA-CP-13-00634* (May 2013).

11. G. F. KNOLL, *Radiation Detection and Measurement*, John Wiley & Sons Inc., New York (2000).

IV. APPENDIX A

An example of the Mg-28 decay chain emission calculation is given in Fig. A.1. For every other calculation the only items that needed to be changed were the material card declaration and the ft8 RES isotope.

Table I. Decay Chains selected for testing.

Decay Chain	Half Life
Mg-28 -> Al-28 -> Si-28	20.9 hrs, 2.2 min, stable
Ar-42 -> K-42 -> Ca-42	32.9 y, 12.36 hr, stable
Cs-137 -> Ba-137m -> Ba-137	30.00 y, 2.55 min, stable
Fe60 -> Co-60 -> Ni-60	1.5e6 y, 5.271 y, stable
Ca-47 -> Sc-47 -> Ti-47	4.536 d, 3.349 d, stable

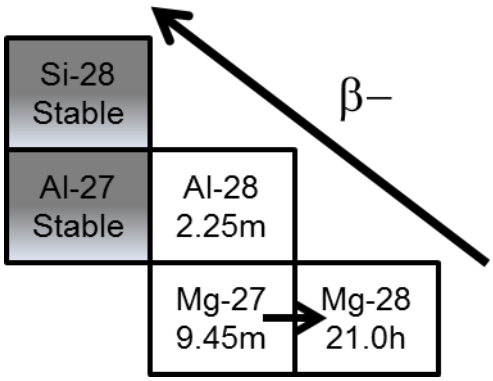

Figure 1. An example decay chain for Mg-28 to Si-28, by way of activation of Mg-27.

Table II. Percent difference between the closed form analytic solutions (A) and the MCNP 1.0 calculations using 1e8 histories (M), given by (M-A)/A*100. The areas labeled NA are due to the fact that the gamma emission is not possible and those lacking a value are due to the fact that gammas were not emitted at that time.

		NPS 1E+08 (Release 1.0)				
Isotope	Lines (eV)	1 min	1 hr	1 day	1 yr	100 yr
Mg-28	3.064E+04	125.1%	126.2%	126.1%	126.1%	126.1%
	4.007E+05	127.2%	126.1%	126.1%	126.1%	126.1%
	9.415E+05	124.7%	126.0%	126.1%	126.1%	126.1%
	1.342E+06	125.3%	126.4%	126.1%	126.2%	126.2%
	1.373E+06	120.3%	126.7%	126.1%	126.2%	126.2%
	1.589E+06	122.7%	126.7%	125.8%	126.1%	126.1%
Al-28	1.779E+06	-42.4%	-42.3%	-42.7%	30.7%	30.7%
Ar-42		NA	NA	NA	NA	NA
K-42	1.525E+06			-47.4%	-54.2%	-53.7%
Cs-137		NA	NA	NA	NA	NA
Ba-137	6.617E+05		-3.7%	-6.0%	-5.6%	-3.3%
Fe-60		NA	NA	NA	NA	NA
Co-60	1.173E+06					-55.1%
	1.333E+06					-55.8%
Ca-47	4.892E+05	48.5%	56.5%	56.8%	56.9%	56.9%
	8.079E+05	66.0%	57.5%	57.1%	57.1%	57.1%
	1.297E+06	55.1%	56.7%	56.9%	56.9%	56.9%
Sc-47	1.594E+05		5.7%	4.0%	49.3%	49.3%

Table III. Percent difference between the closed form analytic solutions (A) and the MCNP 1.0 calculations using 1e9 histories (M), given by (M-A)/A*100. The areas labeled NA are due to the fact that the gamma emission is not possible and those lacking a value are due to the fact that gammas were not emitted at that time.

		NPS 1E+09 (Release 1.0)				
Isotope	Lines (eV)	1 min	1 hr	1 day	1 yr	100 yr
Mg-28	3.064E+04	126.1%	126.1%	126.1%	126.1%	126.1%
	4.007E+05	126.4%	126.2%	126.1%	126.1%	126.1%
	9.415E+05	126.2%	126.1%	126.1%	126.1%	126.1%
	1.342E+06	125.9%	126.1%	126.1%	126.1%	126.1%
	1.373E+06	126.5%	126.1%	126.1%	126.2%	126.2%
	1.589E+06	125.1%	126.1%	126.1%	126.1%	126.1%
Al-28	1.779E+06	-42.3%	-42.2%	-42.4%	31.2%	31.2%
Ar-42		NA	NA	NA	NA	NA
K-42	1.525E+06		-41.8%	-51.1%	-52.4%	-51.8%
Cs-137	0.000E+00	NA	NA	NA	NA	NA
Ba-137	6.617E+05	22.3%	-4.3%	-5.0%	-5.5%	-3.3%
Fe-60		NA	NA	NA	NA	NA
Co-60	1.173E+06				-57.9%	-58.4%
	1.333E+06					-57.1%
Ca-47	4.892E+05	58.1%	57.0%	56.9%	56.9%	56.9%
	8.079E+05	57.9%	57.1%	56.9%	56.9%	56.9%
	1.297E+06	56.8%	56.9%	56.9%	56.9%	56.9%
Sc-47	1.594E+05	3.5%	6.4%	4.0%	49.3%	49.3%

Table IV. Percent difference between the closed form analytic solutions (A) and the MCNP 1.1 calculations using 1e 8th histories (M), given by (M-A)/A*100. The areas labeled NA are due to the fact that the gamma emission is not possible and those lacking a value are due to the fact that gammas were not emitted at that time.

		DBCN 10th Entry (Release 1.1)				
Isotope	Lines (eV)	1 min	1 hr	1 day	1 yr	100 yr
Mg-28	3.064E+04	2.8%	2.9%	2.8%	2.8%	2.8%
	4.007E+05	4.5%	2.9%	2.8%	2.8%	2.8%
	9.415E+05	0.9%	2.7%	2.8%	2.9%	2.9%
	1.342E+06	2.5%	2.8%	2.9%	2.9%	2.9%
	1.373E+06	0.2%	3.2%	2.8%	2.8%	2.8%
	1.589E+06	2.3%	3.1%	2.6%	2.8%	2.8%
Al-28	1.779E+06	-41.2%	-39.5%	-39.4%	-37.6%	-37.6%
Ar-42		NA	NA	NA	NA	NA
K-42	1.525E+06			-55.6%	-57.4%	-56.9%
Cs-137		NA	NA	NA	NA	NA
Ba-137	6.617E+05		-0.6%	-5.8%	-5.3%	-4.0%
Fe-60		NA	NA	NA	NA	NA
Co-60	1.173E+06					-56.0%
	1.333E+06					-53.7%
Ca-47	4.892E+05	1.9%	4.1%	4.4%	4.4%	4.4%
	8.079E+05	9.4%	4.9%	4.6%	4.5%	4.5%
	1.297E+06	2.6%	4.2%	4.4%	4.4%	4.4%
Sc-47	1.594E+05		0.4%	0.1%	4.6%	4.6%

```
Mg_28 Decay Chain
c cell cards
1 1 -1e-6 -1 imp:n 1
2 0        1 imp:n 0

c surface cards
1 so 1e-6

c data cards
m1 12027 1.0
sdef par=n erg=1
mode n p #
ACT  FISSION=NONE
     NONFISSION=P
     DG=LINES
nps 1e8
LCA 7j -2
DBCN 9j 1.6d16
f1:p 1
t1 1e3 6e9         $1 minute
e1 0 5999i 6
f11:p 1
t11 1e3 3.6e11     $1 hour
e11 0 5999i 6
f21:p 1
t21 1e3 8.64e12    $1 day
e21 0 5999i 6
f31:p 1
t31 1e3 3.1536e15  $1 year
e31 0 5999i 6
f41:p 1
t41 1e3 3.1536e17 $100 years
e41 0 5999i 6
f8:# 1
ft8 RES 12028
print
```

Figure A.1. An example MCNP6 Mg-28 decay chain emission calculation.